Improvement of state-resolved kinetic models applied to N_2-CH_4 hypersonic entry flows

João Vargas (n.68460)[1]

[1]*Departamento de Física, Instituto Superior Técnico, Universidade de Lisboa, Lisboa, Portugal*

I. INTRODUCTION

In 1997, the Cassini-Huygens spacecraft was launched from Earth for an interplanetary voyage to Saturn. Arriving in 2004, the Huygens probe detached from the spacecraft and successfully entered the atmosphere of Titan, composed of 98% N_2 and 2% CH_4 mixture. It was the first time a spacecraft landed on an outer Solar System object. Before this, several studies were carried out in order to study the entry point of the spacecraft at 5.15 km/s. It was feared that the high radiation from the CN molecule, previously unaccounted for, would lead to excessive heating of the spacecraft during descent. At this time, models were developed and created around the 5.15 km/s entry point. The result was Gökçen's kinetic scheme [5] which was implemented in the aerothermal database of the Huygens spacecraft.

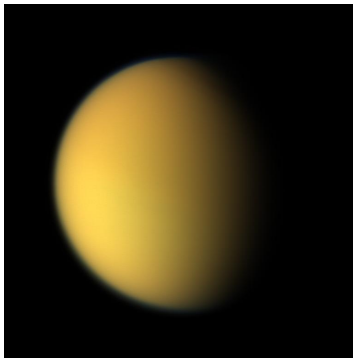

Figure 1: Real color photo of Titan. Credit: NASA.

It was later verified by Lino da Silva *et al.* that not all the rates in the kinetic scheme developed by Gökçen were physically consistent for high temperatures [9]. A new physically consistent kinetic scheme was then proposed by the same authors. Since there is still interest in future missions to Titan, experiments in shock tube facilities of N_2-CH_4 mixtures have been carried out as recently as in 2009 [7]. It is then our objective to put this new kinetic model to the test by comparing it with the older model, and to apply these to the modeling of the most recent experimental results available. However before doing this, some changes had to be made to our in-house thermodynamical and kinetic models. The objectives of this work are then twofold:

- To improve and assess the influence of changes introduced into the thermodynamical and kinetic models of IST's aerothermodynamics code SPARK,
- To compare the modified Gökçen and Lino da Silva kinetic models and to apply the results to the simulation of post-shock radiation in a shock tube.

The modifications we are introducing to both kinetic schemes are of a state-specific nature in order to produce meaningful comparisons between models and the experimental results. Our main tool to achieve this objective is the SPARK code, the in-house code of aerothermodynamics of IST. Also used extensively is the Gas and Plasma Radiation database (GASPAR) mantained by IPFN-GEDG.

II. THEORY AND MODELS

A. Hydrodynamics

A temporal relaxation sub-system is extracted from the full set of conservative equations by neglecting the spatial derivatives, transport terms and setting the gas velocity to zero [2]:

$$\frac{\partial}{\partial t}\begin{bmatrix} c_i \\ T \end{bmatrix} = \frac{1}{\rho}\begin{bmatrix} \dot{\omega}_i \\ \left(\dot{\Omega} - \sum \varepsilon_i \dot{\omega}_i\right)/C_{\mathrm{V}}^{\mathrm{f}} \end{bmatrix} \tag{1}$$

Such a zero-dimensional system allows the study of thermo-chemical relaxation processes occurring in a gas which is suddenly heated to a given temperature keeping the pressure constant. Note that this situation is similar to a entry flow in which the upstream gas is suddenly heated to very high temperatures as it crosses the shock wave. As a result, this temporal system represents a very powerful, yet simple, set of equations to study the relaxation processes occurring in complex atmospheric entry flows.

B. Kinetics

The mass source term reads:

$$\dot{\omega}_i = M_i \sum_r \Delta\nu_{ir}\left[k_{\mathrm{f},r}\prod_i x_i^{\nu'_{ir}} - k_{\mathrm{b},r}\prod_i x_i^{\nu''_{ir}}\right] \tag{2}$$

where ν'_{ir} and ν''_{ir} are the reactant and product stoichiometric coefficients, $\Delta\nu_{ir} = \nu''_{ir} - \nu'_{ir}$ and

$x_i = \rho_i/M_i$ is the molar concentration of species i. The rate constants $k_{\mathrm{f},r}$ and $k_{\mathrm{b},r}$ are associated to the forward and backward processes of the r reaction and are a function of temperature only. The forward reaction rate $k_{\mathrm{f},r}$ is computed through known models associated in a database to each reaction, while the backward rate $k_{\mathrm{b},r}$ is computed through the equilibrium constant $K_{\mathrm{eq}}(T)$:

$$k_{\mathrm{b}}(T) = k_{\mathrm{f}}(T)/K_{\mathrm{eq}}(T), \tag{3}$$

which ensures physical consistency between the forward and the backward rates. The equilibrium constant is computed through the partition functions of the species in a reaction,

$$K_{\mathrm{eq}} = \prod_{i}^{N_s} \left(Q^{\mathrm{tot}}\right)^{\Delta\nu_{ir}}, \tag{4}$$

where the total partition is the product of the translational and the internal partition functions.

C. Thermodynamics

When studying microscopic phenomena, such as radiation and relaxation processes, it is important to account for the internal states of species. In equilibrium, a species follows a Boltzmann distribution of it's internal levels. As a consequence only one mass conservation equation is necessary to describe a chemical species. In non-equilibrium conditions, no distribution can be assumed *a priori*. The occupation levels of each species must then be individually tracked to distinguish between the species states. This is carried out in a so-called state-to-state kinetic approach with a different mass conservation equation for each internal level.

If the electronic levels are allowed to depart from a Boltzmann distribution function then a new mass conservation equation associated to each electronic level is added to the system. The kinetic and radiative processes are now related to the electronic levels and not the chemical species. Notice that the vibrational levels of each molecule are still following the Boltzmann distribution at a given temperature. Relaxing this assumption, each vibronic state needs to be individually described by a mass conservation equation. The collisional and radiative processes now involve the vibrational levels. The rotational levels of a molecule are still following a Boltzmann distribution. The next step would be to relax this assumption and create a kinetic scheme which allows for rotational interactions. This is outside the scope of this work.

The nomenclature utilized throughout this work is as follows: a Boltzmann simulation accounts only for the flow chemical species following a Boltzmann distribution, an electronic state specific (ESS) accounts for some molecular species electronic levels and a vibrational state specific simulation (VSS) accounts for the vibronic states of some chemical species (specifically, only N_2 which accounts for most of the gas composition).

1. Partition function

The internal partition function of a species has contributions from its three different modes: rotation, vibration and electronic. Generically, the partition function of a mode is computed through

$$Q \equiv \sum_s Q_s \equiv \sum_s g_s \exp\left(-\beta\epsilon_s\right), \tag{5}$$

where $\beta = 1/kT$, s is the number of energy levels in the mode, g_s the degeneracy of each level and ϵ_s the energy of level s. The exact computation of this partition function may be carried out using an extensive database detailing the degeneracy and energy of the levels of each mode. If possible or necessary, the partition function calculation can be replaced with an approximated model, as sometimes it is expensive to compute it analytically. At other times there is no *a priori* knowledge on the overall energy levels of the modes.

Then, for a Boltzmann species the internal partition function is given by

$$Q^{\mathrm{tot}}_{\mathrm{int},i} = Q^{\mathrm{tot}}_{\mathrm{rot},i} \times \left[\sum_v Q_{\mathrm{vib},iv}\right] \times \left[\sum_e Q_{\mathrm{ele},ie}\right]. \tag{6}$$

For an ESS species, the total partition function is the sum of the individual partition functions of a species in one particular energy level e',

$$Q^{\mathrm{tot}}_{\mathrm{int},i} = Q^{\mathrm{tot}}_{\mathrm{rot},i} \times \left[\sum_v Q_{\mathrm{vib},iv}\right] \times Q_{\mathrm{ele},i}. \tag{7}$$

A VSS species must have it's electronic and vibrational energy levels specified, e' and v'. The total partition function is accordingly given by:

$$Q^{\mathrm{tot}}_{\mathrm{int},i} = Q^{\mathrm{tot}}_{\mathrm{rot},i} \times Q_{\mathrm{vib},i} \times Q_{\mathrm{ele},i}. \tag{8}$$

D. Radiation

The energy sink term in system (1) exists only because of radiation. For the typical times of a shock tube experiment, no other heat transfer process can occur that accounts any significant energy exchange. As such, assuming an optically thin gas, the radiated intensity is computed through [8]

$$I_{\mathrm{rad}} = \sum_{i,j} N_i \times A_{ij} \times \Delta E_{ij}, \tag{9}$$

where N_i is the number density, A_{ij} is the Einstein coefficient of the transition and ΔE_{ij} the energy difference between the higher and lower energy levels.

III. IMPROVEMENTS TO THE THEORETICAL MODELS

For the sake of brevity, this extended abstract contains little information on the methodology for the obtainment of these results. Instead, we briefly motivate and summarize each addition/modification of the model and describe it's impact on the system. For more information, consult the full text.

A. Nitrogen dissociation by electron impact

The chemical reaction

$$\mathrm{N_2 + e^- \rightleftarrows 2\,N + e^-}, \tag{10}$$

was missing from Lino da Silva kinetic model. Due to the large concentrations of N_2 in the flow, we should not neglect reactions that can directly impact the population of this species. It was found that this reaction held no impact on the final concentrations of the species involved. It was still included in Lino da Silva's kinetic model for the sake of completeness.

B. Harmonic Oscillator model for electronic excited species

The Harmonic Oscillator model is an approximation for the calculation of the vibrational partition function of an ESS or Boltzmann species. Notice that this approximation is not suitable for a VSS species, since it does not separate the contributions of individual vibrational levels to the species vibrational partition function. Assuming the energy of the vibrational levels are given by an Harmonic Oscillator, the vibrational partition function is given by [1]:

$$Q^{\mathrm{tot}}_{\mathrm{vib},i} = \sum_s Q_{\mathrm{vib},is} = \frac{1}{1 - \exp\left(-\frac{\hbar\omega_e}{kT}\right)}. \tag{11}$$

. This allows for a simpler way of computing the vibrational partition function in contrast with the more complex calculation using the vibrational levels of a species, which might not be available in Spark's database. This model was implemented in Spark's code and a small sensitivity test was conducted in order to determine the impact on the final results. It was found that this change of model doesn't cause much deviation from the calculation using the vibrational levels when these are available. The species which deviated the most is N_2 since the database for the vibrational levels of this species is the most complete in Spark.

C. Spontaneous emission processes

The standard approach to modeling spontaneous emission of a species was to compute the lifetime and it's inverse or to assume that the probability of transition was given by the first Einstein coefficient A_{00} [6]. Both these approaches neglect higher vibrational levels transitions. A temperature dependent *pseudo*-rate was computed for spontaneous emission based on the assumption of a Boltzmann distribution on the vibrational levels and the full Einstein coefficients A_{ij}.

Simulations using both approaches revealed that the standard approach to spontaneous emission overestimated the temperature decrease of the flow by a small amount. The impact of this change is negligible on the global properties of the gas but severely affects the populations of excited electronic levels.

D. Vibrational redistribution of reaction rates

Usually, chemical reaction rates are known globally, *i.e.*, the internal levels of the intervening species follow a Boltzmann distribution. Vibrational state-specific kinetics provides the most accurate description of the kinetic processes in a non-equilibrium gas without any assumption on the distribution of the species internal levels. The downside is that usually, the vibrational state-specific rates are not known. We propose a simple model for expanding global rates to vibrational state-specific rates using the energy gap between products and reactants of a reaction.

This model is not physically consistent, but it is simple and works in a first approximation. We intend to implement a better model in the future based on the work of J. Annaloro [10]. It was found that the global results (temperature, mole fractions) do not change much with the addition of this model to the kinetics but the electronic excited states differ remarkably, shifting the population peak and the magnitude of these excited states. This will have a huge impact on the radiative peak of the flow.

IV. SHOCK TUBE SIMULATIONS

In this section, we present a more detailed summary of this thesis as these are the main results of this work. These results are the direct comparison between Gökçen's and Lino da Silva's kinetic models as well as the experimental results from Brandis PhD thesis [7]. These simulations are done with upstream conditions of $T = 300$ K, $p = 13$ Pa, gas mass composition of 98% N_2 and 2% CH_4, the same conditions as in A. Brandis experiments.

Three shock speeds, 5.15, 7 and 9 km/s were simulated but we only present the results from from the 9 km/s shock here as the results from the 5.15 and 7 km/s are similar for Gökçen and Lino da Silva kinetics.

We point out that to perform these simulations the original kinetic schemes from Gökçen and Lino da Silva were adapted to suit our purposes as needed for Boltzmann, ESS and VSS simulations. To perform ESS simulations, our own rates computed from III C were used for spontaneous emission, but the electronic excitation processes and rates are from Magin's kinetic model [6]. VSS simulations have their vibrational-specific excitation and dissociation rates given by the Forced Harmonic Oscillator model (FHO), detailed in [3].

A. Global results

Figures 2 and 3 plot the macroscopic temperature of the gas is plotted for the shock speeds 5.15 and 9 km/s. Each plot displays Lino da Silva's kinetics in solid lines and Gökçen's kinetics in dashed lines. In these two figures there are some trends to be noticed. First, post-shock cooling is generally slower for the Boltzmann model, followed by the ESS and then VSS models. This is in agreement with state-specific kinetics, as endothermic electronic and vibrational reactions favor energy exchanges in the flow, contributing thus to the absorption of a larger amount of translational energy.

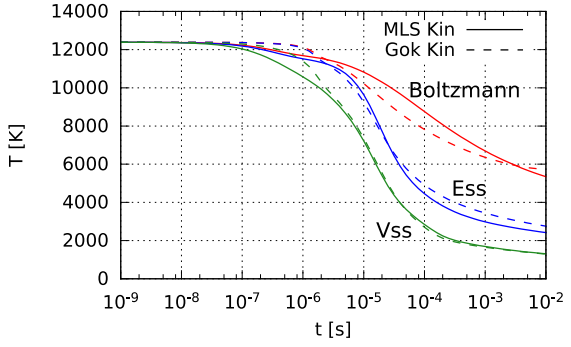

Figure 2: Shock speed of 5150 m/s.

A feature of the 9 km/s shock, is that endothermic processes in Gökçen's kinetics lead to a faster temperature decrease than in Lino da Silva's. In contrast, for a shock of 5.15 km/s, both kinetics agree reasonably on the temperature's values. This outlines the updates of Lino da Silva's from Gökçen kinetics, enforcing the same low temperature behavior but keeping rates physically consistent at higher temperatures. We should therefore expect similar results for low speed shocks at 5.15 km/s but larger discrepancies at 9 km/s.

The dominant difference from the two in kinetics is the dissociation incubation time. As it

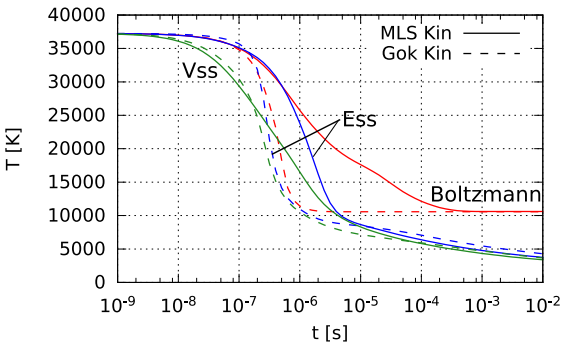

Figure 3: Shock speed of 9000 m/s.

will be corroborated in later figures, dissociation is one of the main endothermic processes. It is clear that for lower shock speeds the temperature starts decreasing later than for higher speeds. The dissociation incubation time is therefore greater for smaller energies, as it would be expected

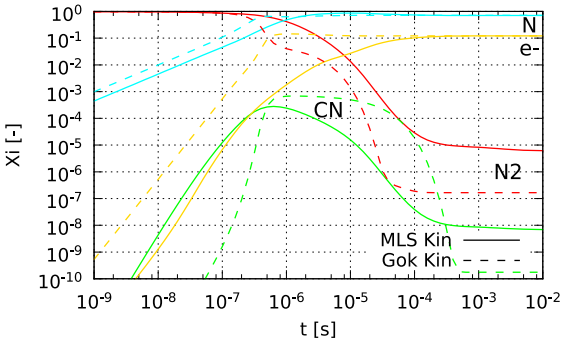

Figure 4: Boltzmann simulation at 9 km/s.

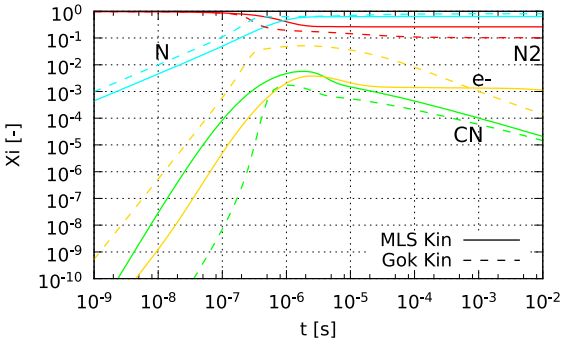

Figure 5: ESS simulation at 9 km/s.

In figures 4, 5 and 6 we plot the mole fractions of selected species for the 9 km/s shock and different kinetic models. The peaks of the N atoms populations are compatible with the temperature decrease in figure 3. Also visible is the decrease of ionization degree (10^{-4}, 10^{-5}, 10^{-6}) as the kinetic model goes from Boltzmann to VSS. This can be explained by the available energy in the flow. Once

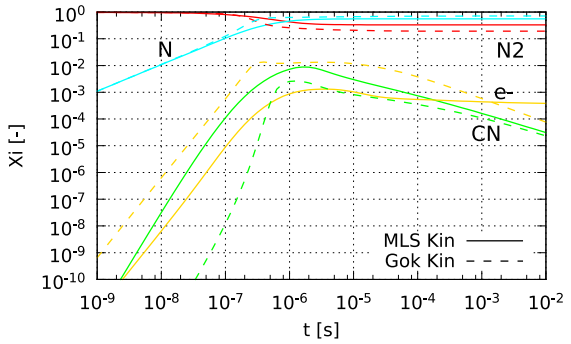

Figure 6: VSS simulation at 9 km/s.

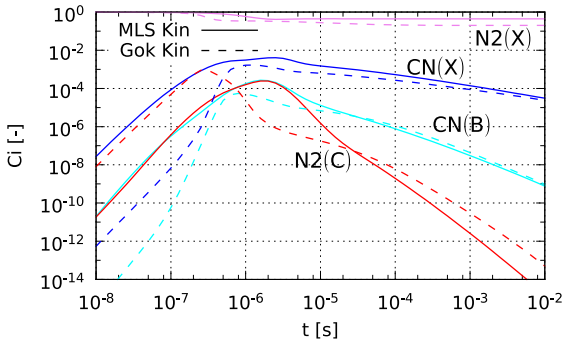

Figure 7: ESS simulation at 9 km/s.

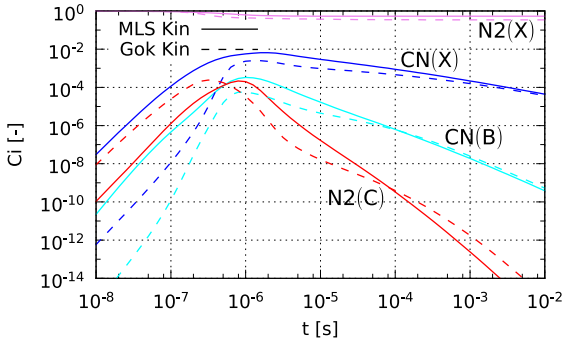

Figure 8: VSS simulation at 9 km/s.

dissociation is fully established, ionization sets in and the more energy is available the higher the ionization degree will be.

The Boltzmann simulation reaches equilibrium conditions around $t = 10^{-3}$, when the molar fractions become constant. This equilibrium is much more pronounced in Gökçen's kinetic scheme probably due to the non-physical rates used in this model which force the gas to reach equilibrium conditions much faster.

We may now draw a more general conclusion on Gökçen's and Lino da Silva's kinetics as well as the kinetic models, Boltzmann, ESS and VSS. Gökçen's kinetics appear to be inadequate at higher temperatures. VSS simulations, include a large number of V-T endothermic processes that the ESS and Boltzmann models are lacking, favoring faster decrease of the plasma temperature downstream of the shock.

B. Excited species populations

In the previous subsection we have showed the unsuitability of Gökçen's kinetics for high temperatures. This subsection is more concerned with the macroscopic properties of the gas. We will be analyzing the populations of the species excited states which are key to the radiative characteristics of the gas.

Radiative processes are intimately linked with these excited electronic states. Figures 7 and 8 plot the mass fraction of stronger emitting species and their corresponding ground levels are shown. At 9 km/s, there is no agreement between the different models and kinetics. The order of magnitude of the peak populations is the same but there is a discrepancy in the time scales across the models. This will have a direct impact on the radiative properties of the gas.

In figures 9 and 10 the vibrational populations time evolution of $N_2(X)$ for Gökçen's and Lino da Silva's kinetic models are plotted for a 9 km/s shock. There is no agreement between the two kinetic models. While the vibrational excitation of $N_2(X)$ is the same (due to the shared FHO model), the higher temperatures reached at this shock speed yield very different N_2 dissociation regimes. A bump in the vibrational distribution for the Gökçen kinetic can be observed around $t = [10^{-7}, 10^{-6}]$. At this time the explanation for this sort of plateau is unclear. We can only speculate that this feature is due to a different interaction of the vibrational redistribution model with the original chemical-kinetic model of Gökçen in comparison to Lino da Silva. In contrast, Lino da Silva kinetics exhibits a smooth temporal evolution.

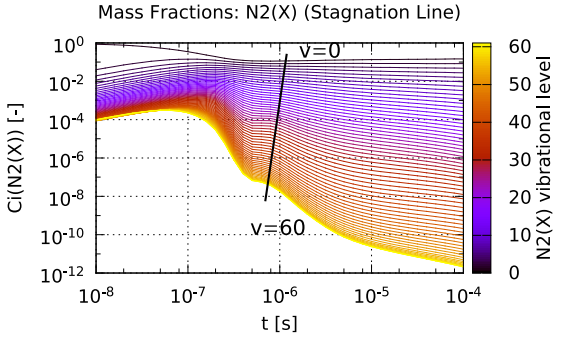

Figure 9: Distribution, Gökçen kinetics at 9 km/s.

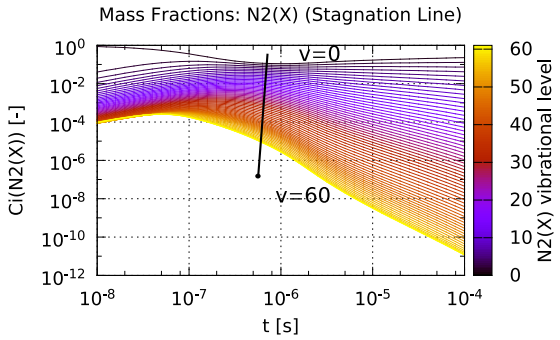

Figure 10: Distribution, Lino da Silva kinetics at 9 km/s.

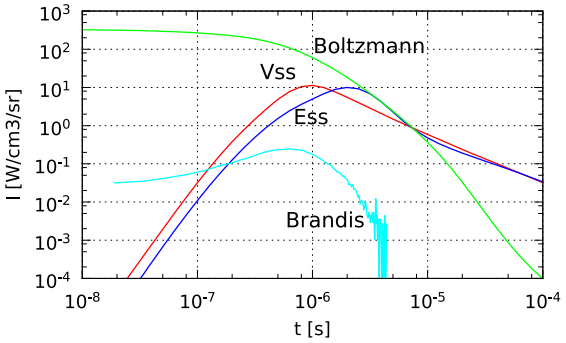

Figure 12: Radiation intensity, Lino da Silva kinetics at 9 km/s.

C. Post-shock radiation

In figures 11 and 12, the post-shock radiative intensity is plotted for Gökçen's and Lino da Silva's kinetic models for the 9 km/s shock speed. The calculated results are compared with experimental data taken from A. Brandis PhD thesis [7]. Note that our simulations are carried out in a 0D framework. Experimental data is not in the same format as a 0D simulation. In fact, experimental data was presented on a distance scale, by considering the distance from the shockwave. The conversion from distance to a time scale is done assuming a constant shock speed. Also, since the spectral window for the shock tube experiments only covers the spectral range $[310, 450]$ nm, the only measured radiation systems are the $N_2(C) \longrightarrow N_2(B)$ (2nd positive) and the $CN(B) \longrightarrow CN(X)$ (violet) systems. This is taken into account in the calculation through a new variable S_{ij} which is 1 if the transition is within the spectral window and 0 if the transition is outside it. S_{ij} is introduced in equation (9).

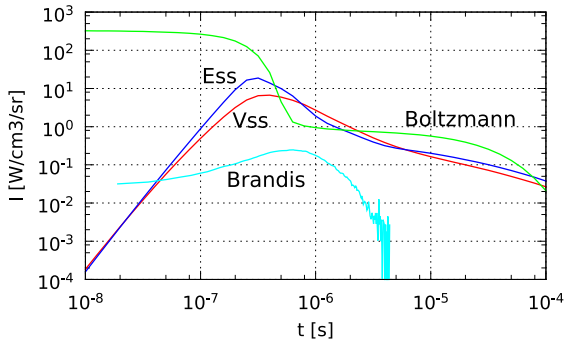

Figure 11: Radiation intensity, Gökçen kinetics at 9 km/s.

The first noticeable difference is that Boltzmann kinetics overpredicts the intensity of radiation. This is expectable since the plasma temperatures is higher for a Boltzmann simulation (see figure 3). Two regimes can also be identified with a change between them at around radiation peak. This is due to the estimation of electronic levels population. The first regime is dominated by the transition $N_2(C) \longrightarrow N_2(B)$ while N_2 is still the majority population. After the radiation peak, CN is mostly created beginning the second regime associated with the dominating $CN(B) \longrightarrow CN(X)$ transition. At 9 km/s, N_2 and CN sufficiently dissociate such that radiation drops with time. This is in agreement with figure 4.

For a 9 km/s shock, ESS and VSS models for each kinetic scheme seem to have different radiative peak heating. The magnitude between simulated results is precise, but not accurate when taking into account the experimental results. The ESS Gökçen predicts a radiative peak sooner, while the ESS Lino da Silva simulation predicts it later when compared with the experiment. The VSS model seems to predict a good radiative peak temporally-wise so. The time of the peak has been better predicted by Lino da Silva, but this result is not yet very satisfactory taking into account the radiative discrepancies in magnitude.

This divergence seems even to be more serious when observing the spectral data from Brandis [7]. N_2 2nd positive system is actually not an observed transition. Yet, it represents an important contribution in the model. This may be due to the lack of a reaction accounting for the dissociation of $N_2(C)$ or a limitation of Magin's kinetic model which is built from data tailored for low temperature plasma experiments. Looking back to figures 7 and 8, the $N_2(C)$ mass fraction presents a relative population similar to the higher vibrational levels of $N_2(X)$ as in figures 9 and 10. If it dissociates as easily as one of the higher vibrational levels, the radiation from the $N_2(C) \longrightarrow N_2(B)$ transition might become negligible. CN(B) doesn't dissociate as well, but globally the dissociation rate of this species is not as high as the dissociation of N_2. Further, dissociation of CN is not occurring before radiation peak but after.

Improvements for the accuracy of this model would be the update of deployed the vibrational

redistribution model. The physical lack of physical consistency of this model has been discussed previously. This model could be improved as in [10] to be physically consistent, hence decreasing the magnitude of the radiation peak. Another factor that could be investigated would be higher shock speed simulations and cross-checking with other experimental data using other initial gas compositions. This could potentially lead to improved model corrections and/or to a better global validation of it.

V. CONCLUSIONS

The two main objectives of this work have been partially achieved. After modifying the kinetic models and simulating the shock tube flows we have reached the following two main conclusions:

- The results for a low shock wave speed are in reasonable agreement with the experimental data. This is not unexpected, since at least Gökçen's kinetic scheme was successfully used to update the aerothermal spacecraft database of the Huygens probe.
- The results for a high shock wave speed are still not satisfactory in magnitude, however the behavior exhibited are reasonable timewise.

We have also stated that further improvements should be made to the kinetic modeling, namely the inclusion in the kinetics for the dissociation of excited electronic states of N_2 and a physically consistent model for the vibrational redistribution. It is expected that these changes will improve the predictive compabilities of the models presented in this thesis.

Acknowledgments

I would like to acknowledge my advisors contributions to this work, Prof. Jorge Loureiro and Prof. Mário Lino da Silva whose counseling have guided and pointed me in the right direction. Although not formally my adviser, Dr. Bruno Lopez was also crucial to the completion of this work with his invaluable help navigating the SPARK code, advice on Fortran programming and all around critic and counselor. This work wouldn't exist without them.

Thanks also to Prof. Vasco Guerra which provided me with already treated data of the cross section of the collision $N_2 + e^-$. Besides these people who have helped me directly, there is also all those who have aided me indirectly. Friends, colleagues and family, to them I would also like to extend my acknowledgments.

[1] J.D. Anderson Jr., *Hypersonic And High Temperature Gas Dynamics Second Edition*, AIAA Education Series, AIAA Reston, Virginia, 2006.

[2] B. Lopez, M. Lino da Silva, V. Guerra, J. Loureiro, *Coupled Hydrodynamic/State-Specific High-Temperature Modeling of Nitrogen Vibrational Excitation and Dissociation*, 44th AIAA Thermophysics Conference, June, AIAA Paper, 2013.

[3] M. Lino da Silva, V. Guerra, J. Loureiro, *State-Resolved Dissociation Rates For Extremely Non-Equilibrium Atmospheric Entries*, Journal of Thermophysics and Heat Transfer AIAA, V.21, N.1, 2007.

[4] G.G. Chernyi, S.A. Losev, S.O. Macheret, B. V. Potapkin, *Physical and Chemical Processes in Gas Dynamics: Cross Sections and Rate Contants* Volume I, Progress in Astronautics and Aeronautics, Volume 196, AIAA Reston, Virginia, 2002.

[5] T. Gökçen, N_2-CH_4-Ar *Chemical Kinetic Model for Simulations of Titan Atmospheric Entry*, Journal of Thermophysics and Heat Transfer AIAA, V21, N.1, 2007.

[6] T.E. Magin, L. Caillaut, A. Bourdon, C.O. Laux, *Non-Equilibrium Radiative Heat Flux Modeling For Huygens Entry Probe*, Journal of Geophysical Research, V.111, 2006.

[7] A. Brandis, *Experimental Study And Modeling of Non-Equilibrium Radiations During Titan and Martian Entry*, PhD Thesis, University of Queensland, 2009.

[8] M. Lino da Silva, D. Tsyhanou, V. Guerra, J. Loureiro, *Simulation of* N_2-CH_4 *Shocked Flows Using a Multiquantum State-to-State Model*, Technical Report, 2011.

[9] M. Lino da Silva, D. Tsyhanou, V. Guerra, J. Loureiro, *A Physically-Consistent Chemical Dataset for the Simulation of* N_2-CH_4 *Shocked Flows Up to* $T = 100000$ *K*, Technical Report, 2011.

[10] J. Annaloro, *Modèles collisionels-radiatifs appliqués aux situations d'entreée atmosphérique martienne et terrestre*, PhD Thesis, University of Rouen, 2013.